Contents List available at VOLKSON PRESS

New Materials and Intelligent Manufacturing (NMIM)

DOI : http://doi.org/10.26480/icnmim.01.2018.94.97

Journal Homepage: https://topicsonchemeng.org.my/

ISBN: 978-1-948012-12-6

PHOTOCATALYTIC REDUCTION OF Cr (VI) by PMo_{12}/TiO_2 ELECTROSPUN NANOFIBER COMPOSITES

Hongfei Shi[1], Chuanbo Dai [1]*, Fang Liu [1], Weidong Wang [1], Huaqiao Tan[2]*

[1]Institute of Petrochemical Technology, Jilin Institute of Chemical Technology, Jilin, 132022, P. R. China.

[2]Key Laboratory of Polyoxometalate Science of Ministry of Education, Faculty of Chemistry, Northeast Normal University, Changchun, 130024, P. R. China.

**Corresponding Author Email: daichb@jlict.edu.cn.; tanhq870@nenu.edu.cn.*

ARTICLE DETAILS

Article History:

Received 26 June 2018
Accepted 2 July 2018
Available online 1 August 2018

ABSTRACT

Polyoxometalates ($H_3PMo_{12}O_{40}$, *abbr.* PMo_{12})/TiO_2 nanofiber composites were fabricated by a facile electrospinning/calcination method. In the structure, PMo_{12}, as an electron relay, can accept the photo-generated electron from the conduction band of TiO_2, which promotes the charge separation. Then the electron stored on PMo_{12} further transfers to the Cr (VI) in the solution to realize the removal of Cr (VI). The PMo_{12}/TiO_2 nanofiber composites exhibit enhanced photocatalytic performance for photocatalytic reduction Cr (VI), which are expected to be one kind of new and environmentally friendly catalyst for removal of inorganic pollutants in water.

KEYWORDS

Polyoxometalates, TiO_2, nanofiber, photocatalysis

1. INTRODUCTION

Over the past few decades, the removal of pollutants from wastewater has received increasing attention. Especially, Cr(VI) can affect human physiology, accumulate in food chain and cause severe health problems ranging from simple skin irritation to lung carcinoma. Contrarily, Cr (III) is low toxic and an essential human nutrient, which does not readily migrate in groundwater since it usually precipitates as hydroxides, oxides, or oxyhydroxides. Therefore, reduction of Cr(VI) to Cr(III) is beneficial for the environment and is a feasible method for removal of Cr(VI) [1].

Recently, photocatalytic removal of toxic substance in aqueous suspension of semiconductor has received considerable attention [2-4]. Among of all the semiconductors, TiO_2 has been widely studied because of its high efficient photocatalytic properties, low cost, nontoxicity, high oxidation ability, chemical stability. Thus, photocatalytic reduction of Cr(VI) over TiO_2 catalysts was extensively investigated [5-7]. However, the relatively wide band gap (~3.2 eV) and low photoinduced charge carrier's separation efficiency hinder its practical application [8]. Therefore, a great deal of efforts has been made to improve the catalytic performances of TiO_2-based photocatalysts, particularly for the morphology engineering, metal or non-metal element doping, sensitizing with dye molecules or narrow band gap semiconductors [9-14].

Spatially separation of the photogenerated charge carriers is a feasible approach for enhancing the photocatalytic performance. Employing an electron scavenger to accept the electron from the conduction band of TiO_2 is an effective way to restrain electron-hole recombination. Polyoxometalates (POMs) are one kind of well-defined early transition metal-oxygen clusters with variety of structures, elemental compositions, and functionalities [15,16]. POMs have reversible redox properties, which can undergo a stepwise multi-electron reversible redox process and their structures have no significant alteration [17]. They exhibit semiconductor-like features with regulated electronic characteristics and energy levels (involving the LUMO and HOMO, corresponding to the CB and VB of semiconductor), and they have been considered as a multielectron acceptors and an ideal candidate to enhance the photocatalytic activity of TiO_2 [18-20]. For POMs-TiO_2 composites, POMs easily accept photogenerated electron from TiO_2 conduction band and electrons are temporarily stored in the form of reduced POMs and later collected electron can be transfer to adsorbed substance. Up to now, although there are a few reports on the high efficiency photodegradation of organic waste, the metal ions waste removal by POMs-TiO_2 composite is rarely reported [21,22].

Herein, we fabricated POMs-TiO_2 composite through a simple and facile electrospinning/calcination method. Firstly, $H_3PMo_{12}O_{40}$ (PMo_{12}) was mixed with polyvinylpyrrolidone (PVP) and titania sol-gel precursor to form PVP-$H_3PMo_{12}O_{40}$-TBT nanofibers by electrospinning. Then the electrospun nanofibers were thermally treated at 400-550°C to remove the PVP and transfer TiO_2 from amorphous to anatase phase. The obtained PMo_{12}/TiO_2 composite exhibits enhanced photocatalytic activity of Cr(VI) reduction. Finally, a proper reaction mechanism of PMo_{12}/TiO_2 working under UV-Vis light irradiation has been proposed.

2. EXPERIMENTAL

2.1 Materials

All chemicals were used without any further purification. Tetrabutyltitanate (TBT), CH_3CH_2OH, $H_3PMo_{12}O_{40}$, C_3H_7OH, CH_3COOH, $K_2Cr_2O_7$ were obtained from Aladdin Chemical Co., Ltd., China. Polyvinylpyrrolidone (PVP, Mw ≈1,300,000) was purchased from *Alfa AesarInc*.

2.2 Preparation of PMo_{12}/TiO_2 nanofiber composites

0.7 g of PVP was dissolved in 15 mL CH_3CH_2OH with vigorous stirring for 3 h to form a clear solution. 0.2 mL CH_3COOH and 0.4 mL TBT were added with stirring. Then calculated amount of $H_3PMo_{12}O_{40}$ (5-30 mol% relative to TBT) was added into the above solution, and it was stirred to form

settled solution. The mixed solution was put into a 20 mL plastic syringe for electrospinning. A 15 kV electrical potential was applied with an electrode distance of 15 cm, and an aluminum foil was used as collector. The solution was ejected at a rate of 0.5 mL·h^{-1} controlled with a syringe pump. The obtained nanofibers were calcined at 400-550°C at a heating rate of 2°C min^{-1} for 5 h in air to remove PVP. TiO_2 nanofibers with different content of PMo_{12} have been fabricated, which are labelled as PMo_{12}/TiO_2 (X Y), Where X and Y values represent the molar ratio of PMo_{12} to TBT and the calcination temperature, respectively. The pure TiO_2 nanofibers without PMo_{12} were prepared as the contrast sample.

2.3 Characterization

The morphology of the sample was observed with a scanning electron microscopy (SEM) on a JEOL JSM 4800F and transmission electron microscopy (TEM, JEM-2100F operated at 200 kV). The crystalline structure was recorded by using an X-ray diffractometer (XRD) (Bruker AXS D8 Focus), using Cu Kα radiation (λ= 1.54056 Å). The UV–Vis absorption spectra were measured on a Shimadzu UV 2600 UV/Vis spectrophotometer. X-ray photoelectron spectrum (XPS) analyses were performed on an ESCALABMKII spectrometer with an Al-Kα (1486.6 eV) achromatic X-ray source.

2.4 Photocatalytic reduction of Cr (VI)

The photocatalytic activity of the samples was evaluated through the reduction of $K_2Cr_2O_7$ in aqueous solution and isopropanol under a 300 W xenon-lamp at a 20 cm distance. Typically, 20 mg of photocatalyst was added into an aqueous solution containing 20 mL of $K_2Cr_2O_7$ solution (160 ppm) and 20 mL isopropanol. The suspensions were stirred in the dark for 0.5 h to obtain absorption-desorption equilibrium between the $K_2Cr_2O_7$ and the catalyst surface before irradiation. Then above mixture was stirred and exposed to the UV-visible-light irradiation. At given irradiation time intervals, about 2 mL of suspension was taken out, centrifuged, and measured at a maximum absorption wavelength of 365 nm.

3. RESULTS AND DISCUSSION

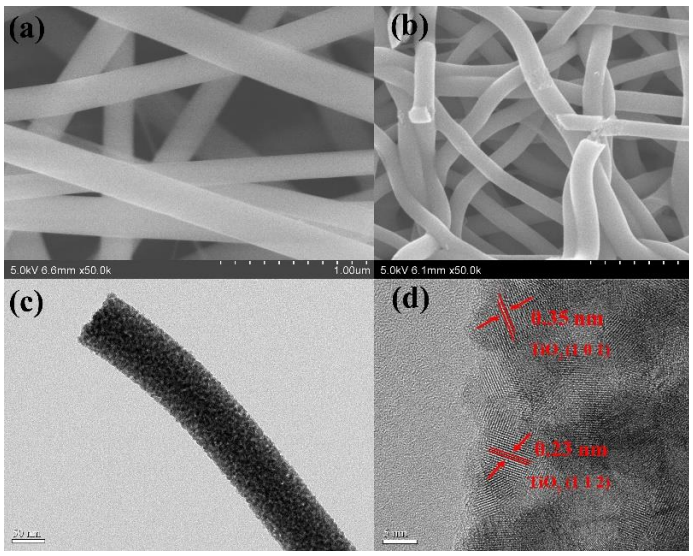

Figure 1: SEM images of PVP/PMo_{12}/TiO_2 (a) and PMo_{12}/TiO_2 (b); TEM photograph of single PMo_{12}/TiO_2 nanofiber (c); HRTEM image of PMo_{12}/TiO_2 fiber(d).

The morphology and microstructure of the PVP/PMo_{12}/TiO_2 nanofibers at the optimum electrospinning conditions (20 mol% Mo/Ti) was illustrated in Figure 1. The nanofibers before calcination exhibit a relative smooth and uniform surface. The fibers are ca. 260 ± 30 nm in diameter and several micrometers in length (Figure 1a). After removing PVP at 450°C, the fibrous morphology of PMo_{12}/TiO_2 is well maintained. As shown in Figure 1b, these fibers become coarse and porous, and the size is reduced to 130±30 nm in diameter.

Figure 1c and 1d present the TEM and HRTEM images of PMo_{12}/TiO_2(20%, 450°C). The TEM image of a single PMo_{12}-TiO_2 nanofiber is shown in Figure 1c. Some dark nanoparticles are observed on the fiber, which may relate to molybdenum existence of PMo_{12}. Figure 1d shows the HRTEM image, the observed lattice spacing of 0.35 nm and 0.23 nm corresponds to the (101) and (112) crystallographic planes of the anatase phase of TiO_2 (JCPDS NO. 21-1272).

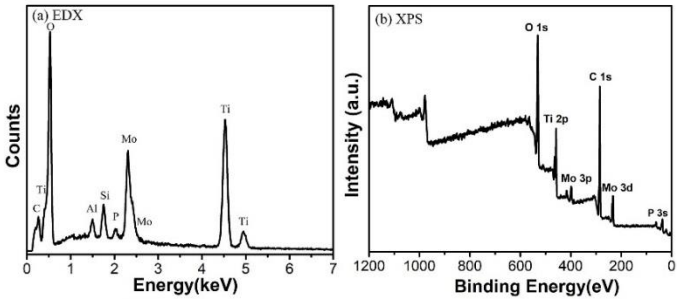

Figure 2: (a) EDX and (b) XPS analysis of PMo_{12}/TiO_2 nanofiber composite.

To further verify the PMo_{12} existence in the fiber, EDX and XPS techniques were employed. Figure 2a clearly exhibits signal of Ti, Mo, O and P elements in EDX pattern of PMo_{12}/TiO_2(20%, 450°C). In Figure 2b, the Mo 3p, Mo 3d, Ti 2p, C 1s, P 3s and O 1s signals are also apparently observed from the full scan survey XPS spectrum of PMo_{12}/TiO_2(20%,450°C) nanofibers. Both EDX and XPS results confirm the formation of PMo_{12}/TiO_2 composite *via* this simple electrospinning/sintering process.

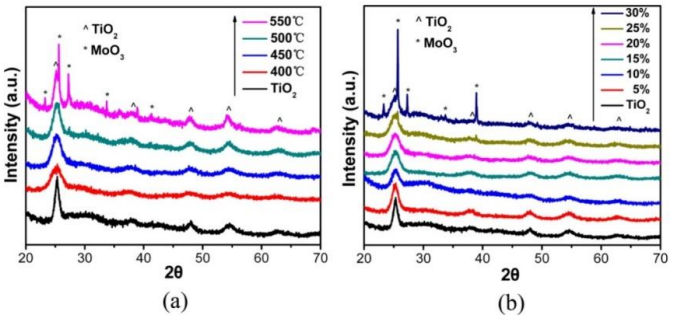

Figure 3: The XRD patterns of (a) PVP/PMo_{12}/TiO_2 (20 mol% Mo/Ti) calcined at different temperature and (b) PVP/ PMo_{12}/TiO_2 with different molar ratio of PMo_{12} to TBT calcined at 450°C.

Figure 3a shows the XRD patterns of PMo_{12}/TiO_2 samples (20 mol% Mo/Ti) with different calcination temperature from 400-550°C. The characteristic diffraction peaks for PMo_{12}/TiO_2, 25.3° (101), 37.8° (004), 48.1° (200), 53.9° (105), 62.7° (204), can be assigned to the crystalline anatase phase of TiO_2 (JCPDS no. 21-1272). The XRD peak at 25.3° turns more and more sharp, indicating the TiO_2 nanoparticle size grows up with the increase of calcining temperature. When the sample was calcined at 550°C, several new diffraction peaks are observed. They match with monoclinic phase MoO_3 (JCPDS no. 05-0508), indicating that PMo_{12} are decomposed to MoO_3 at a higher temperature. Figure 3b shows the XRD patterns of different molar ratio of PMo_{12} to TBT calcined at 450°C. The (101) diffraction peaks of TiO_2/PMo_{12} show wider and lower than pure TiO_2, indicating the addition of PMo_{12} restrain the crystal growth of TiO_2. In addition, the diffraction peaks of MoO_3 are also observed in the 25 mol% and 30 mol% Mo/Ti samples, indicating that PMo_{12} can be also decomposed with a higher amount of PMo_{12}.

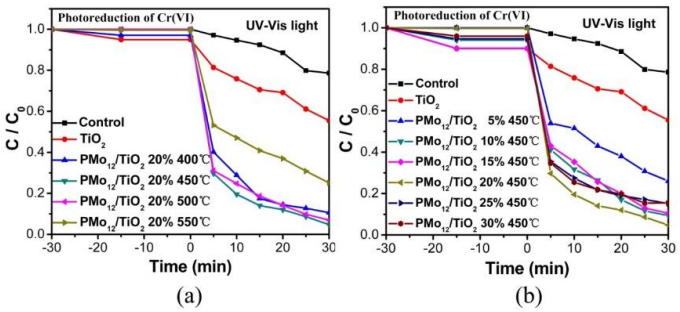

Figure 4: Photocatalytic reduction of Cr(VI) by PMo_{12}/TiO_2 nanofibers prepared at (a) different temperature (20 mol% Mo/Ti) and (b) different feed ratio of PMo_{12} to TBT (calcined at 450°C) under UV-Vis light irradiation. *C* is the concentration of Cr(VI) at time *t*, and C_0 is the concentration of Cr(VI) solution before light irradiation.

Figure 4 shows the time profiles of photoreduction of Cr(VI) for PMo_{12}/TiO_2 prepared with different conditions. An obvious adsorption of Cr(VI) on the nanofibers was observed in all case before irradiation due to their microporous structure. Under the UV-Vis light irradiation, 21.14% of Cr(VI) was photoreduced without catalyst. For pure TiO_2 nanofibers, about 42.16% of Cr(VI) was reduced into Cr(III) in 30 min. The photocatalytic performance of the TiO_2 has been largely improved by the introduction of PMo_{12}. When the molar ratio of PMo_{12} to TBT is 20%, PMo_{12}/TiO_2 450°C shows the best photocatalytic performance. About 96% of 40 mL of 80 ppm Cr(VI) could be photoreduced by 20 mg of photocatalysts (PMo_{12}/TiO_2 20% 450°C) in 30 min. As the calcination temperature was higher than 450°C or the molar ratio of PMo_{12} to TBT was higher than 20%, the polyoxoanion $[PMo_{12}O_{40}]^{3-}$ could be decomposed to MoO_3 as the results of XRD. Therefore, the photocatalytic performances of PMo_{12}/TiO_2 (20% 500°C), PMo_{12}/TiO_2 (20% 550°C), PMo_{12}/TiO_2 (25% 450°C) and PMo_{12}/TiO_2 (30% 450°C) were decreased.

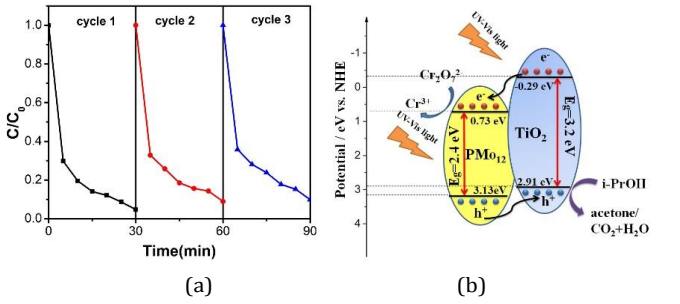

Figure 5: (a)Recycling experiment of photoreduction of Cr(VI) using PMo_{12}/TiO_2 as catalyst. (b)Photocatalytic mechanism of PMo_{12}/TiO_2 composite working under UV-Vis light irradiation.

In Figure 5a, the recycling test reveals the photoreduction efficiency of Cr(VI) shows only a little decrease, which might be attributed to the loss of sample in the recycling process. The result indicates that the PMo_{12}/TiO_2 possesses excellent durability for the removal of Cr(VI).

The LUMO and HOMO value of PMo_{12} is 0.73 V and 3.13 V, which can be calculated *via* cyclic voltammetry and UV-Vis diffuse reflectance spectra methods according to our previous report [23]. Hence, the mechanism of photoreduction of Cr(VI) can be illustrated as Figure 5b. Both of PMo_{12} and TiO_2 can be excited under UV-Vis light irradiation. PMo_{12}, as an electron acceptor, accepts the photogenerated electrons from CB of TiO_2, promoting the charge separation. The electrons can store in the PMo_{12} and then transfer the Cr(VI) ion to produce Cr(III). On the other side, the photo-generated holes can transfer from PMo_{12} to TiO_2 and further to participate in the oxidation reaction with i-PrOH. Consequently, the Cr(VI) was efficiently photoreduced by PMo_{12}/TiO_2 composite.

4. CONCLUSIONS

In summary, PMo_{12}/TiO_2 nanofiber composites were fabricated by a facile electrospinning/calcination method. These composites exhibit highly efficient and recyclable photocatalytic performance for the removal of Cr(VI) under UV-Vis light irradiation, which is ascribed to the effective separation of photogenerated charge carries by the formation of heterojunction between PMo_{12} and TiO_2. This work may provide some new ideas for the design and preparation of new POMs-based photocatalysts with highly efficient photocatalytic performance.

ACKNOWLEDGEMENTS

We acknowledge the financial support from the National Natural Science Foundation of China (21771033).

REFERENCES

[1] Khalil, L.B., Mourad, W.E., Rophael, M.W. 1998. Photocatalytic reduction of environmental pollutant Cr (VI) over some semiconductors under UV/visible light illumination. Applied Catalysis B: Environmental, 17, 267-273. doi: 10.1016/S0926-3373(98)00020-4

[2] Cappelletti, C., Bianchi, C.L., Ardizzone, S. 2008. Nano-titania assisted photoreduction of Cr(VI): The role of the different TiO2 polymorphs. Applied Catalysis B: Environmental, 78, 193-201. doi: 10.1016/j.apcatb.2007.09.022

[3] Gkika, E., Troupis, A., Hiskia, A., Papaconstantinou, E. 2006. Photocatalytic reduction of chromium and oxidation of organics by polyoxometalates. Applied Catalysis B: Environmental, 62, 28-34. doi: 10.1016/j.apcatb.2005.06.012

[4] Liu, X., Pan, L., Lv, T., Zhu, G., Sun, Z., Sun, C. 2011. Microwave-assisted synthesis of CdS–reduced graphene oxide composites for photocatalytic reduction of Cr (VI). Chemical Communications, 2011, 47, 11984. doi:10.1039/C1CC14875C.

[5] Yang, Y., Wang, G., Deng, Q., Ng, D.H., Zhao, H. 2014. Microwave-Assisted Fabrication of Nanoparticulate TiO2 Microspheres for Synergistic Photocatalytic Removal of Cr (VI) and Methyl Orange. ACS applied materials & interfaces, 6, 3008-3015. doi: 10.1021/am405607h

[6] Wang, L., Wang, N., Zhu, L., Yu, H., Tang, H. 2007. Photocatalytic reduction of Cr(VI) over different TiO2 photocatalysts and the effects of dissolved organic species. Journal of Hazardous Materials, 152, 93-99. doi: 10.1016/j.jhazmat.2007.06.063

[7] Colon, G., Hidalgo, M.C., Navio, J.A. 2001. Influence of Carboxylic Acid on the Photocatalytic Reduction of Cr (VI) Using Commercial TiO2. Langmuir, 17, 7174-7177. doi: 10.1021/la010778d

[8] Hoffmann, M., Martin, S., Choi, W., Bahnemann, D. 1995. Environmental Applications of Semiconductor Photocatalysis. Chemical Reviews, 95, 69-96. doi: 10.1021/cr00033a004

[9] Lee, J., Orilall, M., Warren, S., Kamperman, M., Disalvo, F., Wiesner, U. 2008. Direct access to thermally stable and highly crystalline mesoporous transition-metal oxides with uniform pores. Nature Materials, 7, 222-228. doi: 10.1038/nmat2111

[10] Gordon, T., Cargnello, M., Paik, T., Mangolini, F., Weber, R., Fornasiero, P., Murray, C. 2012. Nonaqueous Synthesis of TiO2 Nanocrystals Using TiF4 to Engineer Morphology, Oxygen Vacancy Concentration, and Photocatalytic Activity. Journal of the American Chemical Society, 134, 6751-6761. doi: 10.1021/ja300823a

[11] Zuo, F., Bozhilov, K., Dillon, R., Wang, L., Smith, P., Zhao, X., Bardeen, C., Feng, P. 2012. Active Facets on Titanium (III)-Doped TiO2: An Effective Strategy to Improve the Visible-Light Photocatalytic Activity. Angewandte Chemie International Edition, 51, 6223-6226. doi: 10.1002/ange.201202191

[12] Asahi, R., Morikawa, T., Ohwaki, T., Aoki, K., Taga, Y. 2001. Visible-Light Photocatalysis in Nitrogen-Doped Titanium Oxides. Science, 293, 269-271. doi: 10.1126/science.1061051

[13] Baker, D., Kamat, P. 2009. Photosensitization of TiO2 Nanostructures with CdS Quantum Dots: Particulate versus Tubular Support Architectures. Advanced Functional Materials, 19, 805-811. doi: 10.1002/adfm.200801173

[14] Lu, D., Fang, P., Liu, X., Zhai, S., Li, C., Zhao, X., Ding, J., Xiong, R. 2015. A facile one-pot synthesis of TiO2-based nanosheets loaded with MnxOy nanoparticles with enhanced visible light–driven photocatalytic performance for removal of Cr(VI) or RhB. Applied Catalysis B: Environmental, 179, 558-573. doi: 10.1016/j.apcatb.2015.05.059

[15] Kang, Z., Wang, E., Mao, B., Su, Z., Gao, L., Lian, S., Xu, L. 2005. Controllable Fabrication of Carbon Nanotube and Nanobelt with a Polyoxometalate-Assisted Mild Hydrothermal Process. Journal of the American Chemical Society, 127, 6534-6535. doi: 10.1021/ja051228v

[16] Long, D., Tsunashima, R., Cronin, L. 2010. Polyoxometalates: Building Blocks for Functional Nanoscale Systems. Angewandte Chemie International Edition, 49, 1736-1758. doi: 10.1002/anie.200902483

[17] Sadakane, M., Steckhan, E. 1998. Electrochemical Properties of Polyoxometalates as Electrocatalysts. Chemical Reviews, 98, 219-237. doi: 10.1021/cr960403a

[18] Dolbecq, A., Dumas, E., Mayer, C., Mialane, P. 2010. Hybrid Organic–Inorganic Polyoxometalate Compounds: From Structural Diversity to Applications. Chemical Reviews, 110, 6009-6048. doi: 10.1021/cr1000578.

[19] Du, D., Qin, J., Li, S., Su, Z., Lan, Y. 2014. Recent advances in porous polyoxometalate-based metal–organic framework materials. Chemical Society Reviews, 43, 4615-4632. doi:10.1039/C3CS60404G.

[20] Shi, H., Yan, G., Zhang, Y., Tan, H., Zhou, W., Ma, Y., Li, Y., Chen, W., Wang, E. 2017. Ag/AgxH3–xPMo12O40 Nanowires with Enhanced Visible-Light-Driven Photocatalytic Performance, ACS Appl. Mater. Interfaces, 9, 422-430. doi: 10.1021/acsami.6b13009

[21] Yang, Y., Guo, Y., Hu, C., Jiang, C., Wang, E. 2003. Synergistic effect of Keggin-type [Xn+W11O39] (12−n) − and TiO2 in microporous hybrid materials [Xn+W11O39] (12−n)−−TiO2 for the photocatalytic degradation of textile dyes. Journal of Materials Chemistry, 13, 1686-1694. doi: 10.1039/B212868C

[22] Troupis, A., Hiskia, A., Papaconstantinou, E. 2002. Synthesis of Metal Nanoparticles by Using Polyoxometalates as Photocatalysts and Stabilizers. Angewandte Chemie International Edition, 41, 1911-1914. doi:10.1002/1521-3773(20020603)41

[23] Li, J., Sang, X., Chen, W., Zhang, L., Zhu, Z., Ma, T., Su, Z., Wang, E. 2015. Enhanced Visible Photovoltaic Response of TiO2 Thin Film with an All-Inorganic Donor–Acceptor Type Polyoxometalate. ACS Applied Materials & Interfaces, 7, 13714-13721. doi: 10.1021/acsami.